Title

Application of Black Silicon for Nanostructure-Initiator Mass Spectrometry

Journal

Analytical Chemistry, 88(3)

ISSN

0003-2700

Authors

Gao, Jian

de Raad, Markus

Bowen, Benjamin P

et al.

Publication Date

2016-02-02

DOI

10.1021/acs.analchem.5b03452

Peer reviewed

analytical chemistry

Article

pubs.acs.org/ac

Application of Black Silicon for Nanostructure-Initiator Mass Spectrometry

Jian Gao,[†,‡] Markus de Raad,[†,‡] Benjamin P. Bowen,[†,‡] Ronald N. Zuckermann,[§] and Trent R. Northen*[,†,‡]

[†]Life Sciences Division, Lawrence Berkeley National Laboratory, 1 Cyclotron Road, Berkeley, California 94720, United States

[‡]Joint Genome Institute, Department of Energy, 2800 Mitchell Drive, Walnut Creek, California 94598, United States

[§]The Molecular Foundry, Lawrence Berkeley National Laboratory, 1 Cyclotron Road, Berkeley, California 94720, United States

Supporting Information

ABSTRACT: Nanostructure-initiator mass spectrometry (NIMS) is a matrix-free desorption/ionization technique with high sensitivity for small molecules. Surface preparation has relied on hydrofluoric acid (HF) electrochemical etching which is undesirable given the significant safety controls required in this specialized process. In this study, we examine a conventional and widely used process for producing black silicon based on sulfur hexafluoride/oxygen (SF_6/O_2) inductively coupled plasma (ICP) etching at cryogenic temperatures and we find it to be suitable for NIMS. A systematic study varying parameters in the plasma etching process was performed to understand the relationship of black silicon morphology and its sensitivity as a NIMS substrate. The results suggest that a combination of higher silicon temperature and oxygen flow rate gives rise to the formation of black silicon with fine pillar structures, whose aspect ratio are ~8.7 and depth are <1 μm resulting in higher NIMS sensitivity which is attributed to surface restructuring caused by their low melting point upon laser irradiation. Interestingly, we find selectivity of these black silicon substrates to different analytes depending on the etching parameters. Though, the sensitivity of the dry etching process is lower than the traditional "wet" electrochemical etching process, it is suitable for many applications and is prepared using conventional equipment without the use of HF.

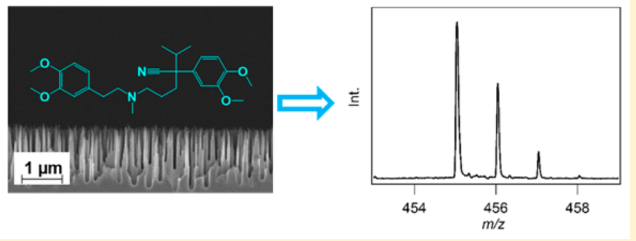

In matrix-assisted laser desorption/ionization (MALDI) mass spectrometry (MS), the efficient cocrystallization process of matrix-analyte is necessary in order to desorb/ionize analytes by energy transfer from the matrix to analytes.[1−4] The anticipated signals of analyte ions (<500 Da) can be buried by high background noise from abundant matrix molecules.[5−7] Matrix-free desorption/ionization is an approach developed to overcome some of the limitations of MALDI, especially for small molecule analysis.[8,9] A great diversity of nanostructured surfaces, such as porous silicon,[10,11] nanopost/nanowire arrays,[12−17] and surfaces with immobilized nanoparticles,[18−20] can be used to support small molecule analysis. Nanostructure-initiator mass spectrometry (NIMS)[21] has high sensitivity and low background of direct analysis of a wide range of samples,[10] such as biofluids, tissues, and single cells.[22−25] NIMS is based on trapping of a liquid "initiator" within the nanostructured surface, which is thought to desorb/ionize from surface during its vaporization with laser irradiation and subsequent heating of the NIMS surface.[21,26]

NIMS sensitivity replies on its nanostructured surface generated by electrochemical etching of highly doped crystalline silicon in a HF bath.[26,27] Since this process involves hazardous chemicals and electric current, it requires extreme caution and safety controls. Even though NIMS has great advantages on analyzing biomolecules (e.g., small molecules, biofluids, tissues, peptides, and cells), the electrochemical etching process has proven to be a significant barrier to the widespread implementation. Therefore, it is desirable to develop an alternative method for fabricating nanostructured surfaces specifically designed for the NIMS technique.

Black silicon is a pillar structured silicon surface with black appearance due to its high antireflectivity of incident light.[28,29] Its efficient light absorption and large surface area makes black silicon attract a wide range of interests, including optoelectronic devices, biomedical devices, and sensors.[30−32] A safe, rapid, controllable method of inductively coupled plasma (ICP) reactive ion etching (RIE) has been developed with high throughput to create black silicon surfaces.[28,33] Thus, black silicon has the potential to replace porous silicon as NIMS substrates owing to its outstanding surface properties and simple fabrication process that does not require HF.

Black silicon surface structures can be controlled by many parameters, such as pressure, temperature, voltage, gas flow rate, and etching time.[28,34−36] Among them, two crucial factors for black silicon formation are gas flow rates and silicon

Received: September 10, 2015
Accepted: January 7, 2016
Published: January 7, 2016

DOI: 10.1021/acs.analchem.5b03452
Anal. Chem. 2016, 88, 1625−1630

temperatures.[34,36,37] An inductively coupled plasma mixture of SF_6 and O_2 gas is generally used. The SF_6 chemically etches the silicon surface by producing volatile SiF_4 while the O_2 produces SiO_yF_x passivation layers, which lead to anisotropic etching and are essential for black silicon formation.[28,37−39] This passivation layer is significantly influenced by silicon temperatures.[36,37,39] Fine tuning of these etching parameters is necessary to produce silicon surface structures that support NIMS analysis.

In this study, we optimized black silicon as NIMS surface for the first time, and these surfaces were produced by a conventional ICP etching process of SF_6 and O_2 gas mixture. A systematic investigation was performed to understand the relationship of black silicon morphology and its sensitivity as a NIMS substrate. Black silicon surface structures were adjusted by varying gas flow rates, etching time, and silicon temperatures, and their relative NIMS activity was characterized using a variety of molecules. These results not only describe a specific approach of preparing NIMS surface but also provide insights of the morphology-sensitivity relationships of black silicon NIMS substrates and help further design black silicon surface structures with high NIMS sensitivity.

EXPERIMENTAL SECTION

NIMS Substrates Fabrication with Black Silicon. Silicon wafers (4 in., p-type doping, 525 ± 25 μm thickness, ⟨100⟩ orientation, 0.01−0.02 Ω cm, purchased from Addison Engineering) were etched by the ICP-RIE process (Oxford Instrument PlasmaLab 100) at cryogenic temperatures. The power was fixed at 5 W for the etching chamber and 1000 W for the plasma generator chamber. Black silicon substrates were obtained in a plasma mixture of SF_6 and O_2 gas at 6 mTorr chamber pressure. Then they were fully soaked with the initiator BisF17 for 40 min and can be used as NIMS substrates after blowing off excess initiator.

Sample Preparation. Spermidine, arginine, adenosine, palmitoylcarnitine, verapamil were purchased from Sigma-Aldrich and STAL-2 (hexapeptide, SFLLRN-NH2) was purchased from AnaSpec. A chemical library with 118 secondary metabolites was obtained from Enzo Life Sciences. All compounds were of high purity grade and their concentration is included in the discussion session. Bradykinin is from a peptide mass standard kit that was purchased from AnaSpec. It is a premixed sample and the concentration used in this study is fixed. Methanol (J. T. Baker, LC−MS grade) and water (J. T. Baker, LC−MS grade) are mixed together following a 1:1 volume ratio (1:9 volume ratio for the limit of detection experiment) as solvent with the additive of 0.1% formic acid (Sigma-Aldrich, MS grade).

Acoustic Printing and NIMS Measurements. Samples were spotted onto NIMS chips using an acoustic printer (EDC ATS-100) with a 10 nL deposition volume. An AB Sciex TOF/TOF 5800 MALDI mass spectrometry system combined with MALDI MSI 4800 imaging software was used for NIMS mass spectrum collection and imaging, and this system was configured for the measurements in the positive ionization mode. The acquired data was analyzed using the OpenMSI program.[40]

RESULTS AND DISCUSSION

A systematic study was performed to understand the correlation of black silicon morphologies and their performance as NIMS substrates. A series of black silicon substrates with different microstructures were obtained by controlling plasma etching conditions, including SF_6/O_2 gas flow rates, etching time, and silicon temperatures. At least three replicas of black silicon under the same etching conditions were prepared to confirm the reproducibility of their surface structures (Supporting Information). The surface morphologies were evaluated using scanning electron microscopy (SEM), and the NIMS sensitivities were based on mass spectrometry of diverse substrates. From this, the morphology-sensitivity relationship was examined to identify parameters improving the NIMS performance.

Morphology-Dependent NIMS Sensitivity. *SF_6/O_2 Gas Flow Rates.* The SF_6/O_2 gas flow ratios are varied from 1 to 11.5 by adjusting the SF_6 flow rate from 20 to 46 sccm and O_2 from 20 to 4 sccm. Figure 1 shows SEM images in cross-section views of these black silicon substrates obtained at fixed etching times. As discussed in the literature,[28,33,37] oxygen amounts in the SF_6/O_2 ICP etching process determine the formation of the SiO_yF_x passivation layer at cryogenic temperatures, which is a key factor of generating the black silicon surface since it makes anisotropic etching profiles possible. As shown in Figure 1, black silicon is not formed when the O_2 flow rate is above 20 or below 4 sccm (Figure 1A,F respectively). Meanwhile, SF_6 concentration plays a crucial role on the etching rate, which controls the formation speed of black silicon.[28] Figure 1A shows the black silicon microstructures grow slowly at SF_6/O_2 20/20 sccm/sccm flow rates due to the limited etching rate caused by this low SF_6 content.

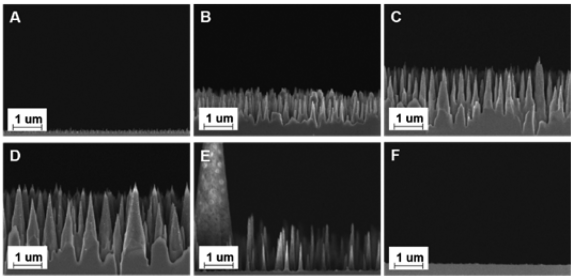

Figure 1. SEM images with cross-sectional views of black silicon surfaces obtained at different SF_6/O_2 gas flow ratios: (A) 20/20, (B) 34/16, (C) 38/12, (D) 40/10, (E) 42/8, and (F) 46/4 sccm/sccm. All these wafers are etched for 5 min at −120 °C.

The typical silicon pillar structures with triangular sloped surface are clearly observed from samples etched at 34/16 to 42/8 sccm/sccm of SF_6/O_2 gas flow rates (Figure 1B−E). Their dimensions are varied with SF_6/O_2 ratios and their heights are within 1 μm scale up to 10 μm. This morphology is dramatically different comparing with the electrochemically etched surface (Supporting Information), and somewhat like the NALDI (nanowire-assisted laser desorption and ionization) surfaces with single crystal nanowires[41] and NAPA (nanopost arrays) produced by e-beam lithography.[16] However, we do find that these nanostructured surfaces trap the "initiator" consistent with the underlying concept of NIMS. Specifically, excess initiator is removed using a jet of nitrogen as typical in preparation of conventional NIMS surfaces. This results in surfaces without visible initiator surface film. As found with the electrochemically etched surfaces, we observe reversible migration of the initiator out of the surface with slight heating and cooling and enhancement of analyte detection with the presence of the initiator (Supporting Information Movie 1).[26]

DOI: 10.1021/acs.analchem.5b03452
Anal. Chem. 2016, 88, 1625−1630

To our knowledge, this is the first time plasma etching has been used to fabricate these nanostructures as NIMS surfaces and given the wide range of etching parameters, it is likely that many new morphologies can be obtained using this approach. As the traditional NIMS substrates, the initiator is found to enhance the efficiency of analyte desorption/ionization (Supporting Information). However, laser absorption and molecular desorption/ionization processes may differ from the electrochemically etched surfaces. In addition, this plasma etching provides a safer alternative approach that is more compatible with conventional silicon wafer processing.

Imaging mass is used to compare NIMS activities for molecules acoustically printed on the NIMS surface resulting in false color images showing the intensity of the molecules (Figure 2A). Using this approach for comparison of NIMS

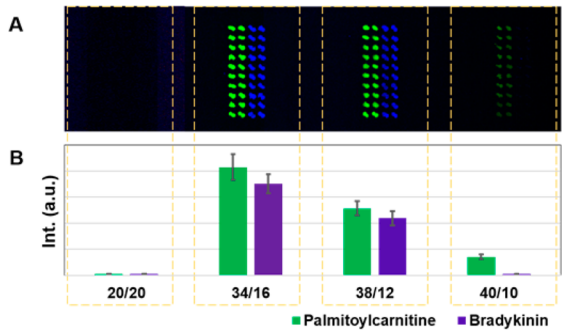

Figure 2. Sensitivity comparison of NIMS substrates prepared with black silicon obtained at different SF_6/O_2 flow rates using mass spectrometry imaging. Palmitoylcarnitine (25 μM, green trace, m/z 400.34 ± 0.01 Da) and bradykinin (blue trace, m/z 905.05 ± 0.01 Da) samples were used here by acoustic printing technique. Panel A shows the direct NIMS imaging results of their sample spots on these black silicon substrates. Panel B shows averaged signal intensities and standard deviations of the image in Panel A (n = 20).

sensitivity, black silicon NIMS substrates prepared with SF_6/O_2 gas flow rates of 20/20, 34/16, 38/12, 40/10 sccm/sccm show a wide range of activities (Figure 2). The black silicon substrate fabricated at SF_6/O_2 34/16 sccm/sccm flow rate shows the highest NIMS sensitivity while the black silicon substrate obtained at SF_6/O_2 20/20 sccm/sccm flow rate appears the lowest NIMS sensitivity for both palmitoylcarnitine and bradykinin samples.

There are many possible explanations for these surface morphology-dependent NIMS sensitivities, such as aspect ratios of silicon pillars, capillary action of initiator, surface areas, and laser absorption efficiency during desorption/ionization process. Since NIMS depends on trapping of liquid initiators to assist analytes desorb from the substrate surface upon laser irradiation,[21,27] so the amount of initiators trapped in the surface may impact NIMS sensitivity. The pillar dimensions of black silicon surfaces generated at SF_6/O_2 20/20 sccm/sccm, which are approximately 100 nm tall, may not be deep enough to hold initiator efficiently resulting in poor NIMS sensitivity. Meanwhile, we speculate that too deep pillar structures, such as black silicon surface fabricated at SF_6/O_2 40/10 sccm/sccm, may trap analytes into pillar forests resulting in low NIMS signals. Importantly, large surface areas of NIMS substrates can facilitate energy transfer from substrate to analytes under laser exposure, which can explain the gradual decreases of NIMS sensitivity (Figure 2B) from the substrate obtained at SF_6/O_2 34/16 sccm/sccm to the substrate obtained at SF_6/O_2 40/10 sccm/sccm since the surface area of the former substrate is approximately 4 times larger than that of the latter as estimated.

Etching Time. Etching time was evaluated for its effect on black silicon morphologies. The gas flow rate was fixed at SF_6/O_2 34/16 sccm/sccm since black silicon generated at this gas rate shows higher NIMS sensitivity comparing with other flow rates used in Figure 2, and etching time is varied from 2 to 5 min. Figure 3 shows the SEM images with cross-section views

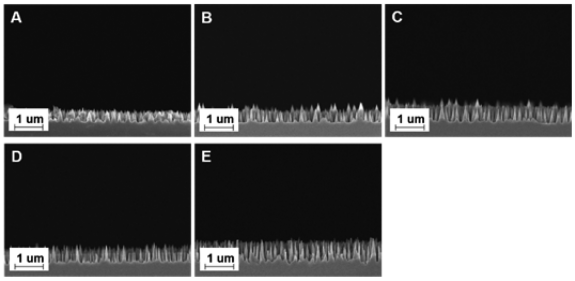

Figure 3. SEM images with cross-sectional view of black silicon surfaces obtained at different etching times: (A) 2, (B) 2.5, (C) 3, (D) 3.5, (E) 5 min. All these wafers are etched at −120 °C with constant SF_6/O_2 gas flow rate of 36/14 sccm/sccm.

of these black silicon substrates. The height of silicon pillars is increased from 250 to 700 nm when etching time is increased to 5 min. It is also observed that silicon pillars appear more homogeneous and thinner with longer etching time (aspect ratios increasing from 1.2 to 4).

The NIMS sensitivity of the black silicon substrates obtained at variable etching time was evaluated using arginine, palmitoylcarnitine, and bradykinin. Northen et al. found desorption/ionization on porous silicon (DIOS) is highly dependent on laser intensity because silicon surface restructuring is a driving force for desorbing and ionizing molecules.[42] Hence we also varied laser intensity to examine the effect of black silicon morphologies on NIMS desorption/ionization process. Unfortunately, the instrument interlocks do not allow measurement of the actual intensity and therefore these laser intensities reflect the instrument settings which control the rotation of a gradient neutral density filter and are therefore not linear. The signals of all analytes are increased dramatically when laser intensity is increased (Supporting Information). Laser intensity-dependent surface reorganization is captured by SEM images in both top-view and cross-sectional views (Supporting Information) which show that NIMS ion generation corresponding to SEM observable changes in surface morphology is similar to what was observed with porous silicon.[42]

The mass spectra of each analyte from every substrate in Figure 3 are averaged and their peak intensities are plotted in Figure 4B. Interestingly, each of these molecules show their unique dependencies on the surface morphologies of black silicon. Arginine shows gradual increases of its signal intensity while the signal of palmitoylcarnitine exponentially grows as up to 5 min etching time of NIMS substrates. For bradykinin, its signal rapidly rises and the intensity reaches a maximum using the substrate with 2.5 min etching time. Afterward, bradykinin signal gradually decreases with etching time of substrates. These results indicate the surface structures of black silicon

DOI: 10.1021/acs.analchem.5b03452
Anal. Chem. 2016, 88, 1625−1630

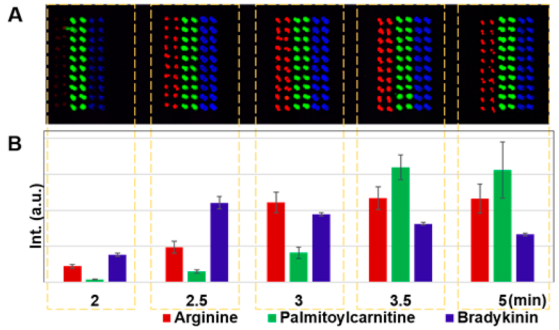

Figure 4. Sensitivity comparison of NIMS substrates prepared with black silicon under variable etching time. Arginine (20 mM, red trace, m/z 175.12 ± 0.01 Da), palmitoylcarnitine (25 μM, green trace), and bradykinin (blue trace) were used and their NIMS imaging results are shown in Panel A. Panel B shows the averaged signal intensities and standard deviations (n = 20).

substrates significantly determine the desorption/ionization process of different analytes.

This surprising finding of selectivity of these black silicon substrates to different analyte molecules is very exciting since it may allow targeting of specific analytes based on surface structures of NIMS substrates. A further study is underway to understand this unique selectivity feature of black silicon NIMS substrates since there is no obvious relationship between the properties of these molecules and their dependence on surface morphologies of black silicon.

Substrate Temperature. The effect of substrate temperature during black silicon formation is also explored by increasing the temperature from −120 °C to −80 °C. At −80 °C, SF_6/O_2 34/16 sccm/sccm gas flow rate, black silicon is formed only when etched for longer than 6.5 min. Figure 5A,B shows the SEM

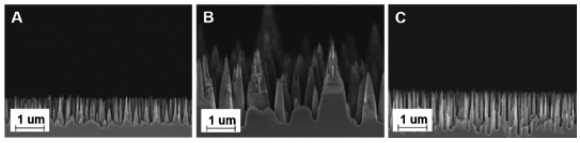

Figure 5. SEM images with cross-sectional view of black silicon surfaces obtained at different conditions: (A) SF_6/O_2 34/16 sccm/sccm, −120 °C, 5 min; (B) SF_6/O_2 34/16 sccm/sccm, −80 °C, 6.5 min; (C) SF_6/O_2 30/20 sccm/sccm, −80 °C, 6.5 min.

images of black silicon substrates fabricated at −120 °C and −80 °C, respectively. The slower black silicon formation rate is attributed to decreased passivation of the SiO_xF_y at higher substrate temperature (−80 °C).[37] Increasing the oxygen concentration compensates for this effect by increasing passivation as shown in Figure 5B,C where oxygen is raised from 16 to 20 sccm with the total gas flow rate fixed at 50 sccm. Therefore, at the higher temperature and oxygen concentration, the silicon pillars appear to be more homogeneous and thinner with the height of ∼1 μm and high aspect ratio of ∼8.7 (Figure 5C) as compared to the low temperature low oxygen concentration (Figure 5A). Resulting in higher surface area and as proposed previously,[42] lower laser intensity is required for gas phase ion generation.

Figure 6 shows the results of NIMS sensitivity measurements of these black silicon substrates using palmitoylcarnitine and bradykinin as analytes. The substrate obtained at −80 °C, SF_6/O_2 34/16 sccm/sccm reveals the lowest sensitivity for both

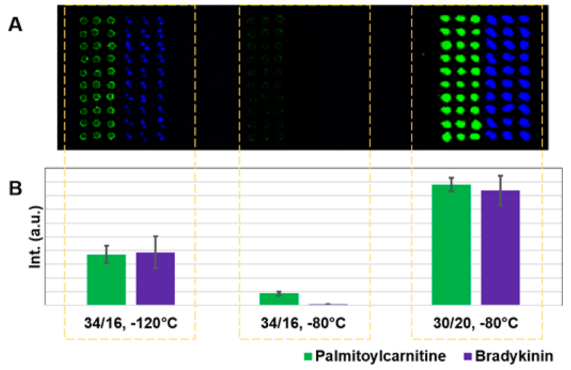

Figure 6. Sensitivity comparison of NIMS substrates prepared with black silicon at different etching temperatures. Palmitoylcarnitine (green trace) and bradykinin (blue trace) samples were used, and their NIMS imaging results are shown in Panel A while averaged signal intensities and standard deviations shown in Panel B (n = 30).

analytes. This low performance could be a combined result of large pillar depth and high melting point of this black silicon substrate. As discussed in sections SF_6/O_2 Gas Flow Rates and Etching Time, its large pillar depth (Figure 5B) can trap analyte molecules and cause its signal decrease, while higher melting point will prohibit its surface restructure and further prevent analytes from desorbing and ionizing from NIMS substrates. The substrate prepared at −80 °C, SF_6/O_2 30/20 sccm/sccm shows strong NIMS signals of both palmitoylcarnitine and bradykinin. The high NIMS sensitivity of this substrate is attributed to its fine vertical pillar structures with the combined features of high aspect ratio and <1 μm pillar depth.

Detection Limit Examination. The NIMS sensitivity of black silicon substrates obtained from the same etching conditions in Figure 5C is further studied using a variety of molecules within a molecule weight range of 100 to 1000 g/mol, including amino acid, lipid, drug, and peptide (spermidine, arginine, adenosine, palmitoylcarnitine, verapamil, STAL-2). The amount of these samples deposited onto the substrates is varied from 10 pmol to 100 fmol by solution dilutions. Correlations of sample amounts and their averaged NIMS signals for each analyte are presented in Figure 7. All of these diverse analytes can be detected via using these NIMS substrates, which demonstrates this type of black silicon NIMS substrate can fit into a wide range of applications.

The signal intensities of spermidine, arginine, adenosine, verapamil, and STAL-2 are proportional to the amount deposited on the substrates. Interestingly, palmitoylcarnitine

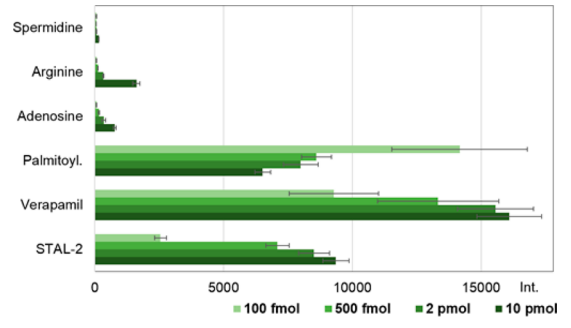

Figure 7. Sensitivity study of black silicon substrates etched for 6.5 min at −80 °C, SF_6/O_2 30/20 sccm/sccm flow rate using a variety of molecules with the amounts of 10 pmol to 100 fmol (n = 5).

DOI: 10.1021/acs.analchem.5b03452
Anal. Chem. 2016, 88, 1625−1630

shows a strange concentration dependence potentially as a result of its amphipathic properties which may enable micelle formation at high concentrations. To more broadly examine the types of compounds that can be detected with reasonable sensitivity, a natural product library containing 118 secondary metabolites was screened with 5 replicates at 250 fmol of each compound using this optimized black silicon NIMS substrate. On the basis of the NIMS imaging results (Supporting Information), ~50% of the compounds were detectable corresponding to their exact mass and ~30% of the compounds showed S/N (signal-to-noise) greater than 5/1. In general, the highest signals were detected from hydrophobic molecules containing protonatable nitrogen atoms.

NIMS substrates from HF electrochemical etching approach have been shown to have extreme sensitivity for verapamil with sensitivity in the yactomole range[10] providing an important benchmark for comparison of this new plasma etching process. We were able to obtain the yactomole sensitivity for verapamil on our TOF/TOF mass spectrometer (Supporting Information). However, the limit of detection for verapamil on the most sensitive black silicon surface (6.5 min at −80 °C, SF_6/O_2 30/20 sccm/sccm) was many orders of magnitude higher (attomole level, Figure 8). Although this value is much higher

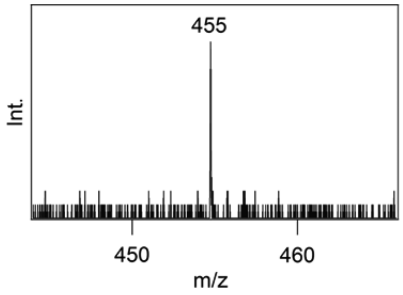

Figure 8. Mass spectrum of 10 amol of verapamil spotted on a black silicon NIMS substrate (SF_6/O_2 30/20 sccm/sccm, −80 °C, 6.5 min). Single laser shot (2000 laser power) is used here.

than that of the electrochemically etched surfaces (Supporting Information),[10] many applications do not require such high sensitivity and the benefit of preparing surfaces using standard plasma etching equipment that does not require custom equipment and use of HF will outweigh this loss of sensitivity. We also anticipate that the sensitivity of the plasma etched surfaces can be further increased given the large parameter space in the ICP etching process.

CONCLUSION

In summary, ICP "dry" etching is demonstrated to be a new method for preparation of NIMS substrates and its sensitivity is highly determined by surface structures. The morphologies of black silicon can be adjusted by varying parameters during ICP etching process. It is found that silicon pillars on black silicon surface should reach a balanced value to absorb enough initiators without preventing analyte molecules desorbing from surface via deep traps, and large surface areas can efficiently improve NIMS sensitivity owing to enhanced energy transfer from substrates to analytes. The laser intensity dependent NIMS signal indicates surface restructuring of black silicon substrates plays an important role on desorption/ionization process of analyte molecules and substrates with fine and high aspect ratio pillar structures show highest NIMS sensitivity, which can be explained by their low melting point. While these surfaces have lower sensitivity for verapamil than electrochemically etched surfaces, the ability to prepare these surfaces without custom fixtures and the use of HF is desirable for many applications and we hope will enable any group with access to an ICP instrument to make NIMS surfaces. The intriguing and yet unexplained analyte specific relationship between surface morphologies and ion detection is currently being examined and has potential to enable fabrication surfaces with enhanced sensitivity for specific molecules. While this work is focused on NIMS analysis of pure compounds in positive instrument polarity, it will be of interest to extend this work to mixtures and negative mode analysis. Finally, since this dry etching process is a common clean-room approach, it has great potential for integration of NIMS capabilities onto microdevices.

ASSOCIATED CONTENT

Supporting Information

The Supporting Information is available free of charge on the ACS Publications Web site. Movie 1 (.avi) records the . The Supporting Information is available free of charge on the ACS Publications website at DOI: 10.1021/acs.analchem.5b03452.

Additional experimental data (PDF)

Movie of the process of initiator coming out from the black silicon NIMS surface with thermal heating (AVI)

AUTHOR INFORMATION

Corresponding Author

*E-mail: TRNorthen@lbl.gov.

Notes

The authors declare no competing financial interest.

ACKNOWLEDGMENTS

This work is supported by Defense Advanced Research Projects Agency (DARPA) Fold F(x) program. Work at the Molecular Foundry was supported by the Office of Science, Office of Basic Energy Sciences, of the U.S. Department of Energy under Contract No. DE-AC02-05CH11231.

REFERENCES

(1) Bizzini, A.; Greub, G. *Clin. Microbiol. Infect.* **2010**, *16*, 1614.
(2) Calderaro, A.; Arcangeletti, M.-C.; Rodighiero, I.; Buttrini, M.; Gorrini, C.; Motta, F.; Germini, D.; Medici, M.-C.; Chezzi, C.; De Conto, F. *Sci. Rep.* **2014**, *4*, 6803.
(3) Marvin, L. F.; Roberts, M. A.; Fay, L. B. *Clin. Chim. Acta* **2003**, *337*, 11.
(4) Harvey, D. J. *Mass Spectrom. Rev.* **2015**, *34*, 268.
(5) Zhang, S.; Liu, J. a.; Chen, Y.; Xiong, S.; Wang, G.; Chen, J.; Yang, G. *J. Am. Soc. Mass Spectrom.* **2010**, *21*, 154.
(6) Schlosser, G.; Pocsfalvi, G.; Huszár, E.; Malorni, A.; Hudecz, F. *J. Mass Spectrom.* **2005**, *40*, 1590.
(7) Duncan, M. W.; Roder, H.; Hunsucker, S. W. *Briefings Funct. Genomics Proteomics* **2008**, *7*, 355.
(8) Peterson, D. S. *Mass Spectrom. Rev.* **2007**, *26*, 19.
(9) Rainer, M.; Qureshi, M.; Bonn, G. *Anal. Bioanal. Chem.* **2011**, *400*, 2281.
(10) Kurczy, M.; Northen, T.; Trauger, S.; Siuzdak, G. In *Mass Spectrometry Imaging of Small Molecules*; He, L., Ed.; Springer: New York, 2015; Vol. *1203*, p 141.
(11) Wei, J.; Buriak, J. M.; Siuzdak, G. *Nature* **1999**, *399*, 243.
(12) Piret, G.; Drobecq, H.; Coffinier, Y.; Melnyk, O.; Boukherroub, R. *Langmuir* **2010**, *26*, 1354.

DOI: 10.1021/acs.analchem.5b03452
Anal. Chem. 2016, 88, 1625−1630

(13) Go, E. P.; Apon, J. V.; Luo, G.; Saghatelian, A.; Daniels, R. H.; Sahi, V.; Dubrow, R.; Cravatt, B. F.; Vertes, A.; Siuzdak, G. *Anal. Chem.* **2005**, *77*, 1641.
(14) Lo, C.-Y.; Lin, J.-Y.; Chen, W.-Y.; Chen, C.-T.; Chen, Y.-C. *J. Am. Soc. Mass Spectrom.* **2008**, *19*, 1014.
(15) Szunerits, S.; Coffinier, Y.; Boukherroub, R. *Sensors* **2015**, *15*, 12573.
(16) Walker, B. N.; Stolee, J. A.; Pickel, D. L.; Retterer, S. T.; Vertes, A. *J. Phys. Chem. C* **2010**, *114*, 4835.
(17) Kim, J.-I.; Park, J.-M.; Hwang, S.-J.; Kang, M.-J.; Pyun, J.-C. *Anal. Chim. Acta* **2014**, *836*, 53.
(18) Arakawa, R.; Kawasaki, H. *Anal. Sci.* **2010**, *26*, 1229.
(19) Seino, T.; Sato, H.; Yamamoto, A.; Nemoto, A.; Torimura, M.; Tao, H. *Anal. Chem.* **2007**, *79*, 4827.
(20) Ma, R.; Lu, M.; Ding, L.; Ju, H.; Cai, Z. *Chem. - Eur. J.* **2013**, *19*, 102.
(21) Northen, T. R.; Yanes, O.; Northen, M. T.; Marrinucci, D.; Uritboonthai, W.; Apon, J.; Golledge, S. L.; Nordstrom, A.; Siuzdak, G. *Nature* **2007**, *449*, 1033.
(22) Yanes, O.; Woo, H.-K.; Northen, T. R.; Oppenheimer, S. R.; Shriver, L.; Apon, J.; Estrada, M. N.; Potchoiba, M. J.; Steenwyk, R.; Manchester, M.; Siuzdak, G. *Anal. Chem.* **2009**, *81*, 2969.
(23) Calavia, R.; Annanouch, F. E.; Correig, X.; Yanes, O. *J. Proteomics* **2012**, *75*, 5061.
(24) Louie, K. B.; Bowen, B. P.; Cheng, X.; Berleman, J. E.; Chakraborty, R.; Deutschbauer, A.; Arkin, A.; Northen, T. R. *Anal. Chem.* **2013**, *85*, 10856.
(25) Moening, T.; Brown, V.; He, L. In *Mass Spectrometry Imaging of Small Molecules*; He, L., Ed.; Springer: New York, 2015; Vol. *1203*, p 151.
(26) Woo, H.-K.; Northen, T. R.; Yanes, O.; Siuzdak, G. *Nat. Protoc.* **2008**, *3*, 1341.
(27) Louie, K.; Northen, T. In *Mass Spectrometry in Metabolomics*; Raftery, D., Ed.; Springer: New York, 2014; Vol. *1198*, p 313.
(28) Jansen, H.; Boer, M. d.; Legtenberg, R.; Elwenspoek, M. *J. Micromech. Microeng.* **1995**, *5*, 115.
(29) Steglich, M.; Lehr, D.; Ratzsch, S.; Käsebier, T.; Schrempel, F.; Kley, E.-B.; Tünnermann, A. *Laser & Photonics Reviews* **2014**, *8*, L13.
(30) Hsu, C.-H.; Wu, J.-R.; Lu, Y.-T.; Flood, D. J.; Barron, A. R.; Chen, L.-C. *Mater. Sci. Semicond. Process.* **2014**, *25*, 2.
(31) Rahman, A.; Ashraf, A.; Xin, H.; Tong, X.; Sutter, P.; Eisaman, M. D.; Black, C. T. *Nat. Commun.* **2015**, *6*, 5963.
(32) Stubenrauch, M.; Fischer, M.; Kremin, C.; Stoebenau, S.; Albrecht, A.; Nagel, O. *J. Micromech. Microeng.* **2006**, *16*, S82.
(33) Jansen, H. V.; de Boer, M. J.; Unnikrishnan, S.; Louwerse, M. C.; Elwenspoek, M. C. *J. Micromech. Microeng.* **2009**, *19*, 033001.
(34) Jiang, F.; Keating, A.; Martyniuk, M.; Prasad, K.; Faraone, L.; Dell, J. M. *J. Micromech. Microeng.* **2012**, *22*, 095005.
(35) Steglich, M.; Käsebier, T.; Zilk, M.; Pertsch, T.; Kley, E.-B.; Tünnermann, A. *J. Appl. Phys.* **2014**, *116*, 173503.
(36) Nguyen, K. N.; Basset, P.; Marty, F.; Leprince-Wang, Y.; Bourouina, T. *J. Appl. Phys.* **2013**, *113*, 194903.
(37) Dussart, R.; Boufnichel, M.; Marcos, G.; Lefaucheux, P.; Basillais, A.; Benoit, R.; Tillocher, T.; Mellhaoui, X.; Estrade-Szwarckopf, H.; Ranson, P. *J. Micromech. Microeng.* **2004**, *14*, 190.
(38) Yoo, J. S.; Parm, I. O.; Gangopadhyay, U.; Kim, K.; Dhungel, S. K.; Mangalaraj, D.; Yi, J. *Sol. Energy Mater. Sol. Cells* **2006**, *90*, 3085.
(39) de Boer, M. J.; Gardeniers, J. G. E.; Jansen, H. V.; Smulders, E.; Gilde, M. J.; Roelofs, G.; Sasserath, J. N.; Elwenspoek, M. *J. Microelectromech. Syst.* **2002**, *11*, 385.
(40) Rübel, O.; Greiner, A.; Cholia, S.; Louie, K.; Bethel, E. W.; Northen, T. R.; Bowen, B. P. *Anal. Chem.* **2013**, *85*, 10354.
(41) Kang, M.-J.; Pyun, J.-C.; Lee, J.-C.; Choi, Y.-J.; Park, J.-H.; Park, J.-G.; Lee, J.-G.; Choi, H.-J. *Rapid Commun. Mass Spectrom.* **2005**, *19*, 3166.
(42) Northen, T. R.; Woo, H.-K.; Northen, M. T.; Nordström, A.; Uritboonthail, W.; Turner, K. L.; Siuzdak, G. *J. Am. Soc. Mass Spectrom.* **2007**, *18*, 1945.

DOI: 10.1021/acs.analchem.5b03452
Anal. Chem. 2016, 88, 1625−1630